

Solvent-Dependent Dihydrogen/Dihydride Stability for $[\text{Mo}(\text{CO})(\text{Cp}^*)\text{H}_2(\text{PMe}_3)_2]^+[\text{BF}_4]^-$ Determined by Multiple Solvent...Anion...Cation Non-Covalent Interactions

Pavel A. Dub,^[a, b] Natalia V. Belkova,^[b] Oleg A. Filippov,^[b] Jean-Claude Daran,^[a] Lina M. Epstein,^[b] Agustí Lledós,^[c] Elena S. Shubina,^{*, [b]} and Rinaldo Poli^{*, [a, d]}

Abstract: Low-temperature (200 K) protonation of $[\text{Mo}(\text{CO})(\text{Cp}^*)\text{H}(\text{PMe}_3)_2]$ (**1**) by $\text{Et}_2\text{O}\cdot\text{HBF}_4$ gives a different result depending on a subtle solvent change: The dihydrogen complex $[\text{Mo}(\text{CO})(\text{Cp}^*)(\eta^2\text{-H}_2)(\text{PMe}_3)_2]^+$ (**2**) is obtained in THF, whereas the tautomeric classical dihydride $[\text{Mo}(\text{CO})(\text{Cp}^*)(\text{H})_2(\text{PMe}_3)_2]^+$ (**3**) is the only observable product in dichloromethane. Both products were fully characterised (ν_{CO} IR; ^1H , ^{31}P , ^{13}C NMR spectroscopies) at low temperature; they lose H_2 upon warming to 230 K at approximately the same rate (ca. 10^{-3} s^{-1}), with no detection of the non-classical form in CD_2Cl_2 , to generate $[\text{Mo}(\text{CO})-$

$(\text{Cp}^*)(\text{FBF}_3)(\text{PMe}_3)_2]$ (**4**). The latter also slowly decomposes at ambient temperature. One of the decomposition products was crystallised and identified by X-ray crystallography as $[\text{Mo}(\text{CO})(\text{Cp}^*)(\text{FH}\cdots\text{FBF}_3)(\text{PMe}_3)_2]$ (**5**), which features a neutral HF ligand coordinated to the transition metal through the F atom and to the BF_4^- anion through a hydrogen bond. The reason for the

switch in relative stability between **2** and **3** was probed by DFT calculations based on the B3LYP and M05-2X functionals, with inclusion of anion and solvent effects by the conductor-like polarisable continuum model and by explicit consideration of the solvent molecules. Calculations at the MP4(SDQ) and CCSD(T) levels were also carried out for calibration. The calculations reveal the key role of non-covalent anion–solvent interactions, which modulate the anion–cation interaction ultimately altering the energetic balance between the two isomeric forms.

Keywords: density functional calculations • dihydrogen complexes • hydride ligands • molybdenum • noncovalent interactions • solvent effects

Introduction


After the discovery of the first isolable transition-metal-dihydrogen complex by Kubas et al.,^[1] this important class of coordination compounds rapidly became an active field of study.^[2] Together with mono- or polyhydride complexes, dihydrogen complexes play an important role in many homogeneous catalytic processes.^[3–5] The most common methods of generating $\eta^2\text{-H}_2$ complexes are addition of H_2 gas to an unsaturated precursor, ligand displacement by H_2 gas and protonation of a hydride complex,^[6] the last being the simplest and most convenient method. Protonation of neutral hydride compounds most often leads to kinetically controlled proton addition to a metal hydride, which forms either a dihydrogen complex, $[\text{M}(\eta^2\text{-H}_2)]$, or a *cis*-dihydride, $[\text{M}(\text{H})_2]$, depending on the nature of the metal and ligands.^[7,8] Recently, the low-temperature protonation of $[\text{M}(\text{Cp}^*)(\text{dppe})\text{H}]$ was shown to give $[\text{M}(\text{Cp}^*)(\text{dppe})(\eta^2\text{-H}_2)]^+$ for $\text{M}=\text{Fe}^{[9–12]}$ or $\text{Ru}^{[13]}$ and *cis*- $[\text{M}(\text{Cp}^*)(\text{dppe})(\text{H})_2]^+$ for $\text{M}=\text{Os}^{[14]}$. When a $[\text{M}(\eta^2\text{-H}_2)]$ complex is initially formed, its ultimate fate depends on the electronic properties of the metal; it is stable if the metal has suitable Lewis acidity and

[a] P. A. Dub, Dr. J.-C. Daran, Prof. R. Poli
CNRS, LCC (Laboratoire de Chimie de Coordination)
Université de Toulouse; UPS, INPT
205, route de Narbonne, 31077 Toulouse (France)
Fax: (+33) 561-553-003
E-mail: rinaldo.poli@lcc-toulouse.fr

[b] P. A. Dub, Dr. N. V. Belkova, Dr. O. A. Filippov, Prof. L. M. Epstein,
Prof. E. S. Shubina
A. N. Nesmeyanov Institute of Organoelement Compounds
Russian Academy of Sciences
Vavilov Street 28, 119991 Moscow (Russia)

[c] Prof. A. Lledós
Departament de Química, Edifici Cn
Universitat Autònoma de Barcelona
08193 Bellaterra (Spain)

[d] Prof. R. Poli
Institut Universitaire de France
103, boulevard Saint-Michel
75005 Paris (France)

 Supporting information for this article (complete spectroscopic data for compounds **2**, **3** and **4**; low-temperature IR spectra in CH_2Cl_2 and THF; tables and figure of the DFT results; Cartesian coordinates of all optimised structures) is available on the WWW under <http://dx.doi.org/10.1002/chem.200901613>.

π back-bonding ability, it isomerises to a polyhydride structure if the metal is strongly back-donating and it will evolve H_2 if there is insufficient back-donation.

When a neutral hydride complex is protonated, the nature of the solvent may be expected to have a profound effect on the outcome through the effects of polarity (defined herein as the dielectric permittivity) and/or the possible establishment of specific interactions (hydrogen bonding) with the neutral solutes (hydride complex, proton donor) or with the proton-transfer product.^[15] Few previous contributions have specifically addressed solvent effects on the protonation process of neutral hydride complexes. For instance, the low-temperature protonation of $[Ru(Cp^*)(H)_3(PCy_3)]$ by RFOH (hexafluoroisopropanol or perfluoro-*tert*-butanol), which gives $[Ru(Cp^*)(H)_2(\eta^2-H_2)(PCy_3)]^+[ORF]^-$, is assisted by the Freon mixture relative to toluene because of the increase in the dielectric constant upon cooling.^[16] The protonation kinetics of $[W_3(dmpe)_3H_3S_4]^+$ is also affected by the solvent (MeCN vs. CH_2Cl_2).^[17,18] The solvent polarity effect on the proton-transfer thermodynamics and energy barrier has been shown for the protonation of $[Ru(CO)(Cp)H(PCy_3)]$ ^[19] and $[RuH_2(PP_3)]$ ^[20] $[PP_3=P(CH_2CH_2PPh_2)_3]$. For the latter system, the ability of the hydrogen-bond-donating solvent to interfere with the formation of hydrogen bonds in the $[M-H\cdots H-A]$ and $[M(H_2)^+\cdots A^-]$ species was demonstrated. More recently, we have shown that the protonation of $[Mo(Cp^*)(dppe)H_3]$ by CF_3COOH can be directed toward the formation of either $[Mo(Cp^*)(dppe)H_4]^+$ or $[Mo(Cp^*)(dppe)H_2(O_2CCF_3)]$ depending on the ability of the solvent to separate the initially formed $[Mo(Cp^*)(dppe)H_4]^+[CF_3COO]^-$ contact ion pair.^[21]

From those studies it is clear that the proton transfer rate and equilibrium position are sensitive to a complex combination of a variety of interactions, such as hydrogen bonding, ion pairs, electrostatic interactions and so forth. The same forces could influence the preference for the classical versus non-classical isomers, but to date there is no example of such a preference switching due to the conditions. Herein, we report the first direct observation of a solvent influence on the classical versus non-classical nature of the protonation product and a computational study that rationalises this phenomenon.

Results

Proton transfer to compound 1 at low temperatures: A previously reported room-temperature protonation study of $[Mo(CO)(Cp^*)H(PMe_3)_2]$ (**1**) by RCO_2H ($R=H, Me, Et$) was shown^[22] to directly afford $[Mo(CO)(Cp^*)(\eta^1-O_2CR)(PMe_3)_2]$ and H_2 , presumably via an initial (unobserved) intermediate η^2-H_2 complex. We now report our studies of the protonation of **1** by $Et_2O\cdot HBF_4$ at room and low (193 K) temperature in solvents with similar polarities and different coordinating abilities (THF and CH_2Cl_2), by using IR (ν_{CO}) and NMR (1H , $^{31}P\{^1H\}$, $^{13}C\{^1H\}$) spectroscopic methods. Like many other hydride complexes, **1** is not stable in CH_2Cl_2 at

ambient temperature, and slowly undergoes H/Cl exchange (ca. 11 % conversion in 26 h),^[23] but this reaction does not take place at any measurable rate at low temperatures, thereby allowing us to carry out low-temperature studies in this solvent.

Addition of a stoichiometric amount of $Et_2O\cdot HBF_4$ to a pale orange solution of **1** in benzene or THF at ambient temperature results in an immediate colour change to deep purple, and gas is evolved. The 1H and $^{31}P\{^1H\}$ NMR spectra showed complete consumption of the starting material and formation of new nonhydridic products (no resonances upfield of TMS). When $Et_2O\cdot HBF_4$ was added at 200 K in $[D_8]THF$, however, the selective formation of the dihydrogen complex $[Mo(CO)(Cp^*)(\eta^2-H_2)(PMe_3)_2]^+$ (**2**) was observed (Figure 1). This is suggested by the broad shape of

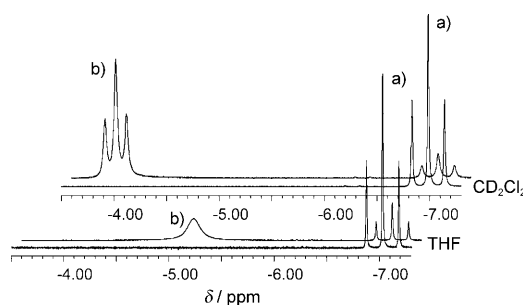


Figure 1. 1H NMR (500 MHz) spectra in $[D_8]THF$ (bottom) or CD_2Cl_2 (top) of a) compound **1** only; b) compound **1** in the presence of slightly less than 1 equivalent of $Et_2O\cdot HBF_4$. $[1]=0.04$ M, $T=200$ K.

the hydride resonance at $\delta=-5.14$ ppm in the 1H NMR spectrum and confirmed by the low T_{1min} value of 24 ms at 190 K (500 MHz). Application of the method of Halpern and co-workers gives an $H-H$ length of 1.1 Å in the slow rotation regime,^[24] or 0.88 Å in the fast rotation regime.^[25] Other selected NMR and IR spectroscopic properties of this compound can be found in Table 1, together with those of the starting material (the complete characterisation is provided in the Supporting Information).

Table 1. Selected NMR and IR spectroscopic data for compounds **1**, **2** and **3** at 200 K.

	Solvent	$\delta_{hydride}^{[a]}$ [ppm]	T_{1min} [ms] (T [K])	$\delta_{PMe_3}^{[b]}$ [ppm]	$\delta_{CO}^{[c]}$ [ppm]	ν_{CO} [cm ⁻¹]
1	$[D_8]THF$	-7.03 (t, 77)	882 (190) ^[d]	32.0 (s)	252.4 (t, 29)	1776
	CD_2Cl_2	-6.98 (t, 77)		31.4 (s)	255.0 (t, 29)	1751
2	$[D_8]THF$	-5.14 (brs)	24 (190)	16.8 (s)	243.9 ^[e]	1852
	CD_2Cl_2	-3.92 (t, 55)	300 (190)	10.0 (s)	231.5 (t, 10)	1954

[a] 1H NMR spectroscopy; multiplicity and $J(H,P)$ [Hz] in parentheses. [b] $^{31}P\{^1H\}$ NMR spectroscopy; multiplicity in parentheses. [c] $^{13}C\{^1H\}$ NMR spectroscopy; multiplicity and $J(C,P)$ [Hz] in parentheses. [d] In $[D_8]toluene$. [e] No information on the multiplicity could be obtained.

A parallel experiment with IR monitoring (ν_{CO} region) showed the growth, after the acid addition, of a new ν_{CO} band at 1852 cm^{-1} , which was attributed to dihydrogen complex **2** (see Figure 2). The high-frequency shift ($\Delta\nu =$

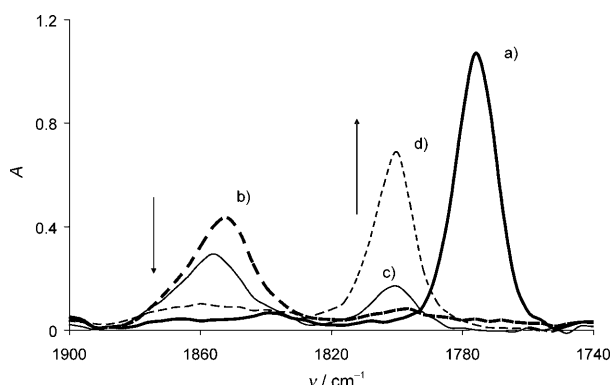
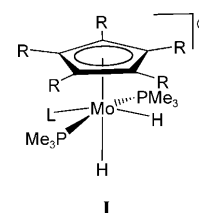


Figure 2. IR spectra of the ν_{CO} region of compound **1** in THF ($C = 1.2 \times 10^{-2}\text{ M}$, $l = 0.4\text{ mm}$, 4 cm^{-1} resolution). a) Alone at 200 K; b) in the presence of $\text{HBF}_4 \cdot \text{Et}_2\text{O}$ (≈ 1 equiv) at 200 K; c) after warming to 230 K (≈ 10 min after spectrum b); d) 3 min after spectrum c).

$+76\text{ cm}^{-1}$) is in accord with a significant lowering of the $\text{M}(\text{d}\pi) \rightarrow \text{CO}(\text{p}\pi^*)$ back-donation upon protonation.^[26] Upon raising the temperature to 230 K, the hydride resonance in the NMR spectrum gradually disappeared whereas H_2 evolved, as shown by the characteristic ^1H NMR signal at $\delta = 4.58\text{ ppm}$. Correspondingly, the intensity of the $\nu_{\text{CO}}(\text{2})$ band in the IR spectrum decreased, and a new ν_{CO} band appeared at 1800 cm^{-1} . The new compound (**4**) is characterised by a $^{31}\text{P}\{^1\text{H}\}$ NMR signal at $\delta = 19.4\text{ ppm}$ and by ^1H NMR signals at $\delta = 1.85\text{ ppm}$ for Cp^* and $\delta = 1.48\text{ ppm}$ for the two PMe_3 ligands at 230 K in $[\text{D}_8]\text{THF}$. No signal was observed for this compound in the hydride region. The nature of this product will be addressed in a later section.

Quite surprisingly, protonation of **1** by $\text{HBF}_4 \cdot \text{Et}_2\text{O}$ in CD_2Cl_2 at 200 K gave completely different spectroscopic changes relative to those in THF (described above), consistent with formation of the dihydride complex $[\text{Mo}(\text{CO})(\text{Cp}^*)(\text{H})_2(\text{PMe}_3)_2]^+$ (**3**; see Figure 1 and Table 1). The hydride ligands exhibit only one triplet signal at $\delta = -3.92\text{ ppm}$ with a $T_{1\rho}$ value of 300 ms at 190 K (500 MHz). A parallel IR experiment revealed a ν_{CO} band for **3** at 1954 cm^{-1} , a much higher frequency ($\Delta\nu_{\text{CO}} = +203\text{ cm}^{-1}$) relative to **2**, in agreement with the formally higher oxidation state in the classical structure. Similar trends in ν_{CO} shifts upon formation of non-classical and classical dihydride derivatives were observed for the protonation of $[\text{Os}(\text{CO})_2(\text{Cp}^*)(\text{H})]$.^[27] The thermal behaviour of **3** is identical to that of **2**: warming the sample to 230 K resulted in H_2 evolution (H_2 signal at $\delta = 4.64\text{ ppm}$) to give **4**. The dihydrogen complex, a possible intermediate in the H_2 evolution process, was not observed in this solvent. To the best of our knowledge, such subtle solvent control of the classical/non-classical equilibrium is unprecedented.

The observation of a single hydride signal for **3** indicates that this compound either adopts a structure with two equivalent hydrides or that they undergo rapid mutual exchange on the NMR timescale. At ambient temperature, the related compounds $[\text{Mo}(\text{Cp})(\text{H})_2(\text{PMe}_3)_3]^+$ and $[\text{Mo}(\text{Cp}^*)(\text{H})_2(\text{PMe}_3)_3]^+$ display averaged resonances that decoalesce at low temperatures, in agreement with structure **1** ($\text{L} = \text{PMe}_3$; $\text{R} = \text{H}$ or Me).^[28,29] Analogous structures were shown by X-ray crystallography for the isoelectronic compounds $[\text{Mo}(\text{Cp})(\text{H})(\text{MeCN})(\text{PMe}_3)_3]^{2+}$, $[\text{W}(\text{CO})(\text{Cp})(\text{H})_2(\text{PMe}_3)_2]^+$ and $[\text{W}(\text{C}_6\text{H}_5\text{Me})(\text{H})_2(\text{PMe}_3)_3]^{2+}$,^[27,28,30] and was also proposed for $[\text{Mo}(\text{CO})(\text{Cp})(\text{dppe})(\text{H})_2]^+$, which, like our complex **3**, only shows one hydride signal at low temperatures.^[31] Therefore, we presume that structure **1** ($\text{L} = \text{CO}$; $\text{R} = \text{Me}$) is also adopted for compound **3**. As will be shown in a later section, the computational work confirms the lower energy of this geometry.



On the basis of the NMR spectroscopy results alone, we could not conclude that the reaction selectively gives a different product in each solvent because rapid interconversion (see the theoretical section below for an estimation of the barrier) would result in a single resonance under all circumstances. However, the much faster IR experiment can distinguish isomers with much shorter lifetimes. No observable IR absorption for non-classical isomer **2** was observed in CH_2Cl_2 (see the Supporting Information, Figure S1) and, likewise, no significant IR intensity for classical isomer **3** was observed in the THF experiment (see the Supporting Information, Figure S2). Given the signal-to-noise ratio of the IR experiment, we can conservatively estimate that $<5\%$ of **2** is present in the CH_2Cl_2 solution of **3** ($K = [\text{2}]/[\text{3}] < 0.053$) and that $<5\%$ of **3** is present in the THF solution of **2** ($K > 24$). This corresponds to a relative stability of the two isomers at 200 K, on the free energy scale, of $>1.1\text{ kcal mol}^{-1}$ in favour of **3** in CH_2Cl_2 and $>1.1\text{ kcal mol}^{-1}$ in favour of **2** in THF.

Other interesting information was obtained from the $^{13}\text{C}\{^1\text{H}\}$ NMR spectra of the protonation products at 200 K. The CO signal moves upfield by $\delta = 8.5\text{ ppm}$ upon transforming **1** to **2**, whereas it moves upfield by $\delta = 23.5\text{ ppm}$ upon transforming **1** to **3**. There is a good correlation between the ^{13}C shifts and ν_{CO} frequencies for these complexes in both THF and CH_2Cl_2 [Eq. (1)] ($r_2 = 0.999$). Such correlations are known for various carbonyl complexes,^[32,33] the ^{13}C NMR shifts and ν_{CO} frequencies being a function of the ligand substituent properties, for example, in complexes with a variety of 4-substituted pyridine ligands $\text{cis}[\text{Mo}(\text{CO})_4(\text{py-4-X})]^{[34]}$ and $[\text{Fe}(\text{CO})(\text{py-4-X})(\text{TPP})]^{[35]}$

$$\delta_{^{13}\text{C}} = -0.116\nu_{\text{CO}} + 458.34 \quad (1)$$

Theoretical study of the factors affecting the dihydrogen-dihydride equilibrium in the $[\text{Mo}(\text{CO})(\text{Cp}^*)(\text{H})_2(\text{PMe}_3)_2]^+$ system: The computational investigation was motivated by a desire to understand the origin of the different isomeric

preference in closely related solvents. All geometry optimisations were carried out by using DFT with both the standard B3LYP functional and the recently introduced^[36] M05-2X functional. The latter has been shown to give better results in studies of non-covalent interactions.^[37] The internal geometries of the Mo complexes are quite functional-independent, the main difference being a systematic shortening of all lengths on going from B3LYP to M05-2X (by ca. 0.05 Å for Mo–P, 0.02 Å for Mo–C_{Cp}, 0.01 Å for Mo–CO and C–O, 0.005 Å for C–C_{ring} and C_{ring}–CH₃). Comparative structural details for the geometries optimised by the two different functionals are available in the Supporting Information (Tables S1–4). Additional calculations on selected systems were carried out by using MP2 and B3PW91 on the fixed B3LYP geometries (Table S5). The structural parameters henceforth reported refer only to the M05-2X calculations.

Of the two possible isomers of **1** with a *cis* or *trans* arrangement of the H and CO ligands, the latter was found to be more stable by $\Delta E^g = -6.6$ kcal mol^{−1}, in agreement with the experimentally suggested geometry. Therefore, only this isomer (Figure 3) was considered in further calculations. Op-

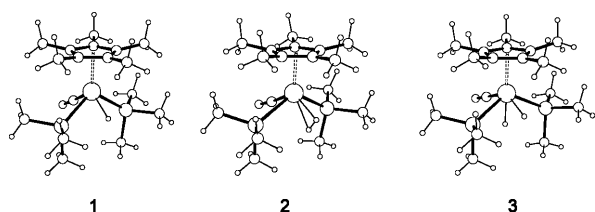


Figure 3. View of the M05-2X optimised geometries of complexes **1**, **2** and **3**.

timisation of non-classical complex **2** revealed two isomers with the H₂ ligand either parallel (see Figure S3 in the Supporting Information) or perpendicular to the Cp* ring (Figure 3). The latter is lower in energy by 0.2 kcal mol^{−1}, but higher by 0.3 kcal mol^{−1} after ZPVE correction and by 0.6 kcal mol^{−1} on the free energy scale. Because most of the non-classical complexes optimised in this work (see below) have the H₂ ligand perpendicular to the Cp* ring, the perpendicular geometry was used as the reference. The energy minimum for classical dihydride **3** corresponds to the expected pseudo-octahedral geometry (see **I**). Other local minima include a second pseudo-octahedral geometry with axial hydride and two *cis* PMe₃ ligands in the equatorial plane (+2.6 kcal mol^{−1} from **I**) and pseudo-pentagonal pyramids with either adjacent or non-adjacent PMe₃ ligands (+5.4 and

+4.1 kcal mol^{−1}, respectively).^[38] The most stable classical geometry of **3** is almost equal in energy to the non-classical isomer **2** in the gas phase (higher by only 1.4 kcal mol^{−1}) and has a low [Mo(η²-H₂)]→[Mo(H)₂] interconversion barrier (4.3 kcal mol^{−1}; see the transition-state geometry in Figure S4). This low barrier is entirely consistent with the minor rearrangement of the coordination sphere during the isomerisation. The proton affinity of hydride **1**, $-\Delta H_{298.15\text{ K}}^g$ for the **1**+H⁺→**2** reaction, is 242.6 kcal mol^{−1}. This gas-phase value gives a first indication of the high basicity of the hydride ligand of **1**.

The effects of the BF₄ counterion and the solvent on the relative stability of **2** and **3** were evaluated by explicitly including the counterion and one or more solvent molecules, and by including the polarisability of the medium through the conductor-like polarisable continuum model CPCM. The results on the relative energy are summarised in Table 2. The individual formation energies relative to the separate cation, anion and solvent in gas phase (ΔE^g) and in solution (ΔE^{soln}) are available in the Supporting Information (Table S6).

Analysis of Table 2 immediately reveals that the chosen models and computational levels do not provide quantitative agreement with the experimental evidence. The DFT methods predict greater stability for the non-classical isomer under all conditions, except for a slight preference for the classical isomer in the case of the gas-phase free cation at the B3PW91 level. The addition of the BF₄[−] anion, or solvent molecule, or both, whether in the gas phase or in the presence of the appropriate CPCM, increase the relative stability of the non-classical isomer, even in CH₂Cl₂, in which a preference for the classical structure is shown experimentally. Conversely, the MP2 method overestimates the stability of the classical isomer. However, all calculations indicate a delicate energetic balance between the two isomers. Note that addition of the solvent, by both explicit inclusion of solvent molecules in the optimisation and consideration of the CPCM, increases the relative stability of the non-classical isomer to a greater extent for THF than for CH₂Cl₂ (for instance the (ion pair)·3CH₂Cl₂ system shows a 5.9 kcal mol^{−1} preference for the non-classical structure, whereas this pref-

Table 2. Relative stability of the dihydrogen and dihydride isomers calculated by using different models.

Model	Gas phase				CPCM (CH ₂ Cl ₂) ^[b]		CPCM (THF) ^[b]	
	ΔE [kcal mol ^{−1}]	ΔG [kcal mol ^{−1}] ^[a]						
cation	M05-2X +1.3 (+1.0)	B3LYP +0.1	B3PW91 ^[c] −1.0	MP2 ^[c] −9.6	M05-2X +2.2 (+1.8)	B3LYP +0.5	M05-2X +2.1 (+1.8)	B3LYP +0.4
cation·CH ₂ Cl ₂	+2.4 (+1.5)	+0.8			+3.2 (+2.4)	+0.7		
cation·THF	+3.2 (+2.3)	+1.1					+3.9 (+3.0)	+0.7
Ion pair	+5.9 (+6.0)	+5.3	+4.6	−4.2	+4.9 (+5.0)	+4.1	+4.8 (+4.9)	+4.0
Ion pair·CH ₂ Cl ₂	+5.5 (+4.2)	+4.5	+3.8	−5.0	+5.5 (+4.1)	+4.2		
Ion pair·THF	+6.9 (+8.0)	+5.5	+4.8	−1.8			+5.9 (+7.0)	+4.2
Ion pair·3CH ₂ Cl ₂	+6.6 (+8.3)				+5.9 (+7.5)			
Ion pair·3THF	+8.8 (+9.5)						+7.4 (+8.1)	

[a] $\Delta E = E_3 - E_2$ and $\Delta G = G_3 - G_2$. [b] The CPCM results were obtained at the fixed geometry from the gas-phase optimisation. The reported values are ΔE^{soln} in kcal mol^{−1}, with ΔG^{soln} in parentheses. The latter have been obtained by adding the gas phase free energy corrections on the solute to ΔE^{soln} . [c] The B3PW91 and MP2 calculations were carried out at the fixed B3LYP-optimised geometry.

erence increases to $7.4 \text{ kcal mol}^{-1}$ for the (ion pair)·3THF system).

All CPCM calculations were carried out on the fixed geometries obtained from the gas-phase optimisation. The possibility that the CPCM might significantly affect the geometry of the energy minimum was tested by fully reoptimising the **2**·BF₄ and **3**·BF₄ geometries (only at the M05-2X level) in the presence of the CH₂Cl₂ and THF CPCM. The internal geometry of the cation was practically unaffected, whereas the cation–anion interactions became slightly looser (slightly longer H···F and shorter B–F hydrogen bond lengths), see Table S4. However, the energy differences in solution were not greatly affected (from +4.9 to +4.9 kcal mol^{−1} in CH₂Cl₂; from +4.8 to +4.6 kcal mol^{−1} in THF). Thus, we wondered whether there may be an inherent bias in favour of the non-classical structure in the DFT method and in favour of the classical structure in MP2.

Geometry optimisations at higher level are prohibitive for this system. Therefore, calibration tests were carried out at the MP4(SDQ) and CCSD(T) levels by using the MP2-optimised geometries of the [Mo(CO)(Cp*)(H)₂(PMe₃)₂]⁺ systems only as free ions in the gas phase, as well as the MP2, B3LYP, B3PW91 and M05-2X levels with full geometry optimisation. These calculations gave the following values for $E_3^s - E_2^s$: +0.1 (B3LYP), −1.0 (B3PW91), +1.3 (M05-2X), −8.4 (MP2), −4.1 (MP4(SDQ)) and −3.7 (CCSD(T)). For this system, the higher-level MP4(SDQ) and CCSD(T) calculations give essentially identical results, which suggests greater stability for dihydride complex by around 3 kcal mol^{−1} relative to the dihydrogen isomer. These results are halfway between those of the DFT methods, which overestimate the stability of the dihydrogen complex by 4–5 kcal mol^{−1}, and that of MP2, which overestimate the stability of the dihydride by the same amount. If this 4–5 kcal mol^{−1} correction is applied to the values shown in Table 2, they then agree well with the experimental observations. Thus, this calibration test is in agreement with the bias of DFT in favour of the non-classical structure and of MP2 in favour of the classical structure.

The remainder of this section will focus on a more detailed analysis of the effects introduced by the anion and solvent on the structure and energetic properties, which should give a clue as to how the solvent operates for switching the cation isomeric preference. The effects of anion and solvent on selected IR spectral parameters (ν_{HH} , ν_{MH} and ν_{CO}) are analysed in the Supporting Information (Tables S7 and 8).

Ion pairing: Calculations show that in the gas phase and in solution the ion-pair interaction dominates over the solvent–cation and solvent–anion interactions, in agreement with the presence of the ion pair in low-polarity solvents, rather than the separated solvated ions (formation energies for cation–solvent, anion–solvent and cation–anion are collected in Table S6). The calculations also demonstrate that the presence of the counterion significantly modifies the classical–non-classical equilibrium in favour of the dihydrogen com-

plex (by $4.5 \text{ kcal mol}^{-1}$ at the M05-2X level and by $5.4 \text{ kcal mol}^{-1}$ at the MP2 level in the gas phase). This effect is probably related to a stronger cation–anion interaction for **2**·BF₄, as suggested by the shorter F···H contacts (see Figure 4). For both **2**·BF₄ and **3**·BF₄, many of these F···H

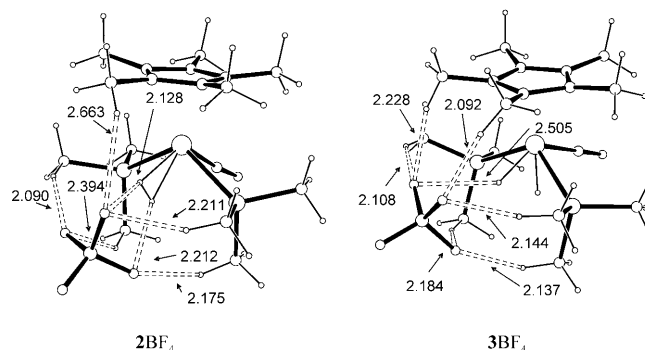


Figure 4. View of the M05-2X-optimised geometries for ion pairs **2**·BF₄ and **3**·BF₄.

plex (by $4.5 \text{ kcal mol}^{-1}$ at the M05-2X level and by $5.4 \text{ kcal mol}^{-1}$ at the MP2 level in the gas phase). This effect is probably related to a stronger cation–anion interaction for **2**·BF₄, as suggested by the shorter F···H contacts (see Figure 4). For both **2**·BF₄ and **3**·BF₄, many of these F···H contacts are substantially shorter than the sum of van der Waals radii (2.55 Å), but those found in **2**·BF₄ are on average shorter than those of **3**·BF₄. Note that F···H separations involving the dihydrogen ligand in **2**·BF₄ are close to the shortest lengths, which implicates the Cp* and PMe₃ hydrogen atoms (ca. 2.1 Å). On the other hand, the F···H(Mo) contacts in **3**·BF₄ ($> 2.3 \text{ Å}$) are longer than the F···H(C) contacts (ca. 2.0 Å ; see Figure 4).

Bulk solvent effects: Calculations prove that the solvent, described as a continuum, plays a minor role in discriminating the two isomers, which could have been anticipated from the very similar dielectric constants (THF $\epsilon = 7.58$; CH₂Cl₂ $\epsilon = 8.93$). Both solvents stabilise **2** by $0.7 \text{ kcal mol}^{-1}$, whereas **2**·BF₄ is disfavoured by $1.0 \text{ kcal mol}^{-1}$ in CH₂Cl₂ and by $1.1 \text{ kcal mol}^{-1}$ in THF (M05-2X values). Although the continuum decreases the preference for **2**·BF₄, ion pairing still provides greater stabilisation to **2**. Of course, depending on the relative stability of the two isomers of the isolated cation, the ion-pair formation in solution will either reverse the energy ordering or not. However, bulk solvent effects alone are not able to explain the different behaviour in THF and CH₂Cl₂.

Discrete solvent effects: The explicit addition of solvent molecule(s) (either CH₂Cl₂ or THF) to the ion-pair model engenders additional non-covalent interactions with the anion, solvent···anion···cation, rather than with the cation, and involves the solvent C–H bonds as proton donors. Therefore, any effect on cation stabilisation must be indirect, through a modulation of the non-covalent cation–anion interaction by the non-covalent solvent–anion interaction(s). The relative cation–anion orientation is only slightly disturbed by the addition of solvent, without significant lengthening the F···H(C) interactions (see Tables S3 and 4 in the Supporting Information), whereas the solvent–anion

(C)H...F interactions are significantly longer (by ca. 0.1 Å for CH₂Cl₂ and by ca. 0.2 Å for THF) than in the absence of the cation (Table S4). No clear trend could be identified in the internal structure of the Mo complexes (classical or non-classical). Both M05-2X and MP2 calculations show that the interaction of the ion-pair with THF stabilises **2**·BF₄[−] (by 1.0 and 2.4 kcal mol^{−1} at the M05-2X and MP2 levels, respectively). The interaction with CH₂Cl₂ has less influence in the relative stabilities and works in favour of **3**·BF₄[−] (by 0.4 and 0.8 kcal mol^{−1} at the M05-2X levels and MP2 levels). These calculations qualitatively reproduce the experimental trends: the dihydrogen complex is favoured in THF and the classical dihydride is favoured in CH₂Cl₂. The inclusion of three THF molecules provides a relative stabilisation of 2.9 kcal mol^{−1} to **2**·BF₄[−], whereas three CH₂Cl₂ molecules only stabilise it by 0.7 kcal mol^{−1}. If the cluster formed by the ion pair and three discrete solvent molecules are solvated with the continuum, the results are only slightly modified.

We conclude that the calculations show that ion-pairing with the BF₄[−] counterion energetically stabilises the dihydrogen complex and the theoretical modelling of the specific solute-solvent interactions suggests that the solvent establishes specific F...H(C) interaction with the anion. The interaction between dichloromethane and the non-classical ion pair [Mo(CO)(Cp*)(η²-H₂)(PMe₃)₂]⁺BF₄[−] destabilises the cation-anion bonding and favours its isomerisation to the dihydride form. On the other hand, the weaker interaction with THF is insufficient to perturb the anion-cation interaction and the non-classical form remains favoured, as in the gas phase. It is arguable that these effects are responsible for the predominance of a different isomer depending on the solvent.

Protonation of compound 1 by CF₃COOD: The protonation of **1** was also investigated in [D₈]THF with CF₃COOD, with the aim of generating complex [D₁]-**2** and measuring the ¹J-(H,D) value. However, ¹H and ³¹P{¹H} NMR spectroscopic monitoring revealed no evidence for the formation of the desired product when using one equivalent of the acid. The only observable species was compound [D]-**1**, which was evidenced by an isotopically shifted ³¹P{¹H} NMR signal at δ = 32.3 ppm (1:1:1 triplet, ²J(P,D) = 10 Hz). When the amount of acid was increased to ten equivalents, the relative intensity of the [D]-**1** ³¹P{¹H} NMR signal increased, which is consistent with a greater extent of H/D exchange at the hydride position, but the signals of **1** in the ¹H and ³¹P{¹H} spectra did not disappear. In addition, a broad and weak signal at δ = −4.5 ppm became visible in the ¹H NMR spectrum (cf. δ = −5.14 ppm for **2**·BF₄[−]). This chemical shift difference can be explained either by a direct counterion effect, presumably through hydrogen bonding (Mo(H₂)...X) on the proton chemical shift, or by an effect of X on the classical/nonclass-

ical equilibrium position. Unfortunately, the resonance intensity was not sufficient for an accurate T_{1 min} determination.

The lower degree of protonation of **1** by CF₃COOD relative to HBF₄ can be explained by the lower acid strength of the former acid. However, reversible protonation of [D₁]-**2** occurs to a sufficient extent to allow the H/D exchange process. Other hydride compounds, for instance [Ru(Cp)H(L₂)] (L₂ = dppe, dppe, 2 PPh₃), have been shown to be protonated by HBF₄ and not by other relatively strong acids such as TFA, HCl or HBr in THF.^[39]

Investigation of the dihydrogen elimination product: As mentioned above, the dihydrogen elimination from **2** in [D₈]THF or **3** in CD₂Cl₂ occurs above 230 K to give solutions with very similar spectroscopic properties, see Table 3.

Table 3. Selected spectroscopic data for the product of H₂ evolution from **2** in [D₈]THF and **3** in CD₂Cl₂ at 230 K.

Solvent	¹ H NMR ^[a]		³¹ P{ ¹ H} NMR ^[a]	¹³ C{ ¹ H} NMR ^[a]	IR
	δ _{Cp*} [ppm]	δ _{PMe₃} ^[b] [ppm]	δ _{PMe₃} ^[c] [ppm]	δ _{CO} ^[d] [ppm]	
[D ₈]THF	1.85 (s)	1.48 (d, 8)	19.4 (quint, 8)	268.7 (t, 31)	1800
CD ₂ Cl ₂	1.88 (s)	1.47 (d, 8)	19.2 (s)	[e]	1794

[a] Signal multiplicity and relevant coupling constants [Hz] in parentheses. [b] J(P,H). [c] J(P,F). [d] J(C,P). [e] Not detected.

When the reaction was carried out in C₆D₆ at room temperature, the ³¹P NMR spectrum showed a major, broader (w_{1/2} = 10 Hz) peak at δ = 17.5 ppm and a minor sharper one at δ = 15.5 ppm (w_{1/2} = 4 Hz). When carried out in [D₈]THF, the broader signal (w_{1/2} = 16 Hz) was observed at δ = 18.1 ppm whereas the sharper one was split into two separate signals at δ = 16.8 and 16.7 ppm in a ratio of about 2:1 (w_{1/2} = 3 and 4 Hz respectively). A solution in THF obtained in the same manner showed a visible absorption with a maximum at λ = 510 nm (ε ≈ 2 × 10² m^{−1} cm^{−1}). The decomposition rate estimated from the IR data at 230 K is essentially the same for **2** in THF and **3** in CH₂Cl₂ (ca. 2 × 10^{−3} s^{−1}), corresponding to an activation free energy ΔG_{H₂}[‡] of 16.2 kcal mol^{−1}. This value is much lower than that obtained for the H₂ loss from [Mo(Cp*)(dppe)(H)₄]⁺[OCOCF₃][−] that gives [Mo(Cp*)(dppe)(H)₂(O₂CCF₃)] (ΔG_{H₂}[‡] = 22.1 kcal mol^{−1} at 270 K).^[21]

Possibilities envisaged for the structure of the product are either [Mo(CO)(Cp*)(L)(PMe₃)₂]⁺[BF₄][−], in which L is the solvent (which implies that the different donor properties of the two solvents affect the spectroscopic properties of the complex only in a minor way), or [Mo(CO)(Cp*)(FBBF₃)(PMe₃)₂], in which the BF₄[−] anion has entered the metal coordination sphere. The first hypothesis seems reasonable for [D₈]THF, which has relatively good coordinating properties, but is less so for CD₂Cl₂. However, note that complexes in which dichloromethane acts as a ligand have been described.^[40,41] The second hypothesis finds precedent in work by Beck et al., who described the formation of the thermolabile complexes [Mo(CO)₂(Cp)(PR₃)(FBBF₃)] (R = Ph, OPh,

Et) as the products of the reaction between $[\text{Mo}(\text{CO})_2(\text{Cp})(\text{H})(\text{PR}_3)]$ and $\text{Ph}_3\text{C}^+\text{BF}_4^-$.^[42] Note that the protonation of hydride complexes is one of many general methods to access metal complexes of weakly coordinating anions, which are precursors of cationic organometallic Lewis acids.^[43]

A most enlightening observation comes from the $^{31}\text{P}\{^1\text{H}\}$ NMR spectrum of the sample obtained in $[\text{D}_8]\text{THF}$, and especially its coupling pattern, which features a perfect binomial quintet ($J = 8 \text{ Hz}$) at 230 K (Figure 5) and coalesces

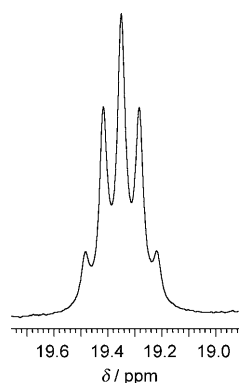
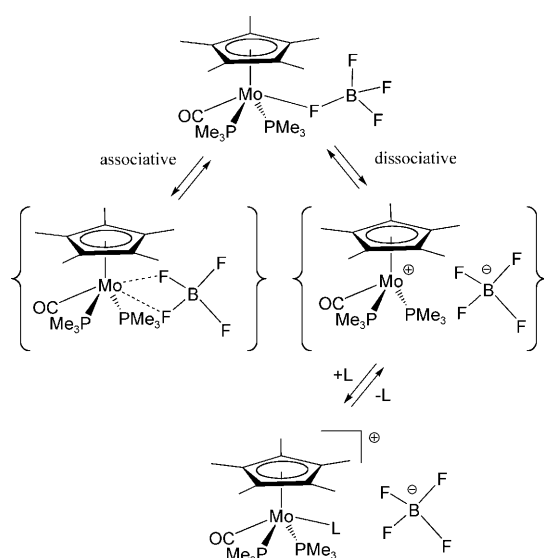


Figure 5. Enlargement of the $^{31}\text{P}\{^1\text{H}\}$ NMR signal for the compound obtained from the decomposition of **2** in $[\text{D}_8]\text{THF}$ at 230 K.

into a singlet at room temperature. The only possible way to rationalise this coupling pattern is to invoke P–F scalar coupling and therefore BF_4^- coordination. However, the observed identical coupling to all F atoms implies a rapid mutual (intramolecular) exchange between the four atoms in the coordination position. This may occur by either an associative or a dissociative mechanism, as shown in Scheme 1. This situation has been previously described for



Scheme 1.

$[\text{W}(\text{CO})_2(\text{Cp})(\text{FBF}_3)\{\text{P}(\text{O}^i\text{Pr})_3\}]$ ^[44] and also for complexes that contain other weakly coordinating anions, such as $[\text{W}(\text{CO})_3(\text{FSbF}_3)(\text{NO})(\text{PMe}_3)]$.^[45] The product of H_2 evolution from either **2** or **3** can, therefore, be formulated as $[\text{Mo}(\text{CO})(\text{Cp}^*)(\text{FBF}_3)(\text{PMe}_3)_2]$ (**4**). There are numerous crystallographically characterised compounds displaying this coordination mode for the BF_4^- ion, mostly with late transition metals. No X-ray structure has so far been reported for mononuclear complexes of Mo^{II} , but related examples for W^{II} include $[\text{W}(\text{CO})_3(\text{FBF}_3)(\text{NO})(\text{PMe}_3)]$ ^[46] and $[\text{W}(\text{CO})_3(\text{FBF}_3)\text{H}(\text{PCy}_3)_2]$.^[47]

Contrary to the behaviour in $[\text{D}_8]\text{THF}$, the $^{31}\text{P}\{^1\text{H}\}$ NMR signal in CD_2Cl_2 is a singlet at all temperatures, consistent with a greater extent of dissociation of the ion pair in this solvent, which is expected to better solvate the BF_4^- ion through the establishment of $\text{F}_3\text{B}-\text{F}\cdots\text{H}-\text{CHCl}_2$ hydrogen bonds^[20,48] (see also the computational work on $2\cdot\text{BF}_4\cdots\text{solvent}$ and $3\cdot\text{BF}_4\cdots\text{solvent}$, described above). This leads to faster intermolecular anion exchange and consequently loss of P–F coupling. However, the similarity of the ν_{CO} frequencies of **4** in the two solvents (Table 3) suggests that the major species present in solution also adopts a molecular geometry in CH_2Cl_2 .

It is interesting to compare the rate of mutual F exchange in **4** with that of similar, previously investigated, compounds, all of which have at least one additional CO ligand in the coordination sphere, for example, $[\text{M}(\text{CO})_2(\text{Cp})(\text{FBF}_3)(\text{L})]$.^[42,44,49] They are most typically at the slow exchange limit at low temperatures and reveal an averaged spectrum only in certain cases at room temperature. In our case, no decoalescence or any sign of line broadening was noticeable down to 190 K. This comparison shows that the BF_4^- ligand is much more labile in compound **4**, probably for both steric and electronic reasons. The collective behaviour of the different compounds appears most consistent with a dissociative exchange mechanism. The shape of this resonance in $[\text{D}_8]\text{THF}$ changes upon warming, becoming a singlet and shifting upfield on going to ambient temperatures ($\Delta\delta = 1.3 \text{ ppm}$ between 230 and 298 K). This behaviour gives evidence for the onset of an exchange that involves more than one ion pair, probably assisted by solvent coordination (as shown in Scheme 1), whereby coupling information between a specific Mo atom and a specific BF_4^- group is lost. Again, this is a typical phenomenon already observed for other FBF_3 complexes.^[43] Therefore, the compound exists at low temperatures in $[\text{D}_8]\text{THF}$ as an uncharged molecular species, perhaps in equilibrium with a tight ion pair (the dissociative intermediate of the mutual exchange process), but equilibrates at higher temperatures with increasing amounts of the free ions, allowing the intermolecular exchange (see Scheme 1).

Formation and characterisation of an HF complex: Leaving solutions of complex **4**, either in $[\text{D}_8]\text{THF}$ or in CD_2Cl_2 , at ambient temperature for extended periods of time resulted in further decomposition. Monitoring by using ^{31}P and ^{13}C NMR spectroscopy revealed the formation of several

products. Upon attempting to crystallise compound **4** prepared in situ from **1** and 0.5 equivalents of $\text{Et}_2\text{O}\cdot\text{HBF}_4$ in toluene at around 250 K, violet crystals were obtained. An X-ray analysis shows that they correspond to $[\text{Mo}(\text{CO})(\text{Cp}^*)(\text{FH}\cdots\text{FBF}_3)(\text{PMe}_3)_2]$ (**5**), that is, the coordination position occupied by the BF_4^- anion in compound **4** has been replaced by a neutral HF molecule, which then further binds to the BF_4^- anion through a hydrogen bond.

Table 4. Selected bond lengths and angles for compound **5**.^[a]

Bond lengths [Å]			
CNT1–Mo1	1.9968(12)	Mo1–P2	2.4777(7)
Mo1–C6	1.895(3)	P1–C113	1.810(3)
C6–O6	1.177(3)	P1–C111	1.815(3)
Mo1–F1	2.2988(16)	P1–C112	1.825(3)
F1–H1A	0.96	P2–C213	1.815(3)
F1–H1B	0.96	P2–C212	1.815(3)
F1⋯F13	2.697(3)	P2–C211	1.825(3)
F1⋯F14	2.714(2)	B1–F11	1.325(4)
H1A⋯F14	1.78	B1–F12	1.362(4)
H1B⋯F13	1.79	B1–F13	1.384(4)
Mo1–P1	2.4672(7)	B1–F14	1.386(4)
Bond angles [°]			
F1–H1A⋯F14	164	F12–B1–F13	106.3(3)
F1–H1B⋯F13	157	CNT1–Mo1–P1	120.11(4)
Mo1–F1–H1A	122.0	CNT1–Mo1–P2	121.71(3)
Mo1–F1–H1B	118.0	Mo1–F1–F14	129.18(8)
Mo1–F1–F13 ⁱ	130.70(9)	CNT1–Mo1–F1	114.96(6)
P1–Mo1–P2	118.07(2)	CNT1–Mo1–C6	117.72(8)
C6–Mo1–F1	127.32(9)	C6–Mo1–P2	74.76(7)
C6–Mo1–P1	74.51(8)	F1–Mo1–P2	78.74(4)
F1–Mo1–P1	79.35(5)	F11–B1–F14	111.4(3)
O6–C6–Mo1	177.4(2)	F12–B1–F14	108.1(2)
F11–B1–F12	110.8(3)	F13–B1–F14	108.2(3)
F11–B1–F13	111.7(3)		

[a] CNT is the Cp ring centroid. Symmetry code: $i = 1-x, 1-y, 1-z$.

Selected bond distances and angles for the structure of compound **5** are listed in Table 4. Each anion makes two short $\text{F}\cdots(\text{HF})$ contacts with two different cations through atoms F13 and F14, and each cation is in close proximity to two different anions, such that the anions and cations are packed in pairs, as shown in Figure 6. Therefore, the proton of the HF ligand must be disordered between two sites, the $\text{F1}\cdots\text{F13}$ and $\text{F1}\cdots\text{F14}$ vectors. The disordered H atom was, in fact, directly located in both positions, with the intensity data suggesting a 50:50 distribution (see details in the Experimental Section). The other two F atoms of the anion, F11 and F12, do not display any contact with neighbouring ions

shorter than the van der Waals distances. The four B–F bonds are not equivalent, with those involved in the hydrogen bond with HF (B1–F13 and B1–F14) being the longest. The structure also contains one molecule of interstitial toluene.

The coordination geometry of the cation is a typical “four-legged piano stool”, with one CO, two PMe_3 and an HF molecule as “leg” ligands. The CNT–Mo–L angles are in the narrow 115–122° range. The most interesting structural feature is the hydrogen-bonding interaction between the ions. Hydrogen bonds connecting two fluorine atoms in coordination compounds are common when the proton acceptor is metal-bound F^- to give the hydrogen bifluoride $(\text{FHF})^-$ ligand, crystallographically characterised examples being $[\text{M}(\text{FHF})(\text{H}_2\text{F})(\text{PMe}_3)_4]$ ($\text{M} = \text{Mo}, \text{W}$),^[50,51] $[\text{Ru}(\text{dppe})_2(\text{F})(\text{FHF})]$,^[52] $[\text{Ru}(\text{FHF})(\text{H})(\text{PMe}_3)_4]$,^[53] $[\text{Rh}(\text{cod})(\text{FHF})(\text{PPh}_3)]$ ($\text{cod} = \text{cyclooctadiene}$)^[54] and $[\text{Pd}(\text{FHF})(\text{Ph})(\text{PPh}_3)_2]$.^[55] However, we found no precedent in the CSD of an HF ligand bonded to a transition metal with an additional hydrogen bond to BF_4^- . In the structures in which the H atom was located (see above), this is placed closer to the dangling F atom than to the metal-coordinated F atom. The structure can, therefore, be better represented as an HF adduct of a fluoro complex, $\text{M–F}\cdots\text{H–F}$, rather than a cationic HF complex, $[\text{M}(\text{F–H})]^+\cdots\text{F}^-$, whereas the disordered H atom in **5** is located closer to the molybdenum bound F atom than to FBF_3 (0.96 vs. 1.78 Å), allowing this compound to be better described as a cationic HF complex, $[\text{Mo}(\text{CO})(\text{Cp}^*)(\text{FH})(\text{PMe}_3)_2]^+\cdots\text{FBF}_3^-$. The Mo–F bond in **5** is much longer than the typical terminal $\text{Mo}^{\text{II}}\text{–F}$ bond to a fluoro ligand (average of 2.01(4) Å over nine bonds in seven structures retrieved from the CDS).^[56–62] The above-mentioned $[\text{Mo}(\text{FHF})(\text{H}_2\text{F})(\text{PMe}_3)_4]$ complex also has a shorter Mo–(FHF) bond (2.124(3) Å) than our compound because the fluorine atom bonded to Mo has a greater electron density in $(\text{FHF})^-$ relative to $(\text{FH}\cdots\text{FBF}_3)^-$. The closest relative to the arrangement of the HF ligand in the structure of **5** is

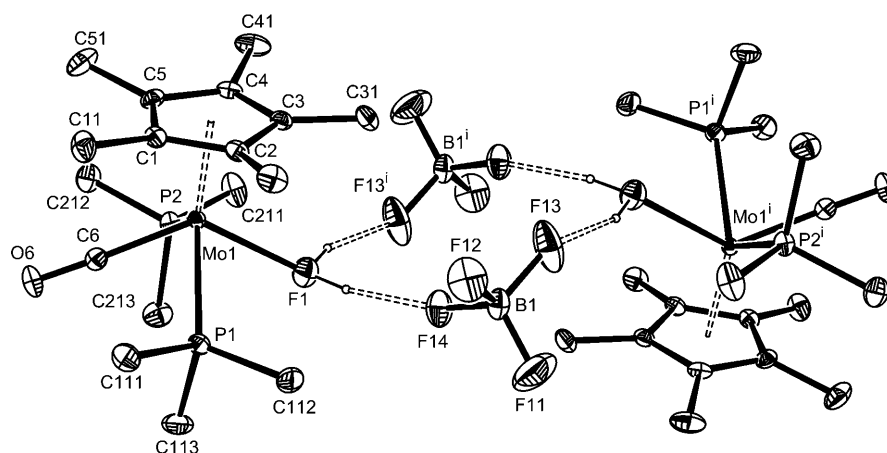


Figure 6. An ORTEP view of the molecular geometry of $[\text{Mo}(\text{CO})(\text{Cp}^*)(\text{FH}\cdots\text{FBF}_3)(\text{PMe}_3)_2]$ (**5**) (with an atom-labelling scheme) that shows the formation of a pseudo-dimer through $\text{F–H}\cdots\text{F}$ hydrogen bonds. Displacement ellipsoids are drawn at the 30% probability level and the disordered H atoms are represented as small spheres of arbitrary radius. Symmetry code: $i = 1-x, 1-y, 1-z$.

[La(HF)₂(AsF₅)₃], in which intermolecular La–(FH)⋯(FAsF₅)La is observed.^[63] It should be mentioned that intramolecular examples of M–(FH)⋯B moieties (B = proton acceptor, such as the 2-NH₂ group of metal-coordinated *o*-aminopyridine) have also been described, though without structural characterisation.^[64,65] Comparison of all these results shows that with a proton acceptor as strong as F[−] there is a preference for M–F⋯H–F, whereas weaker proton donors (neutral NH₂ groups or anionic AsF₆[−] and BF₄[−]) lead to M–F–H⋯B.

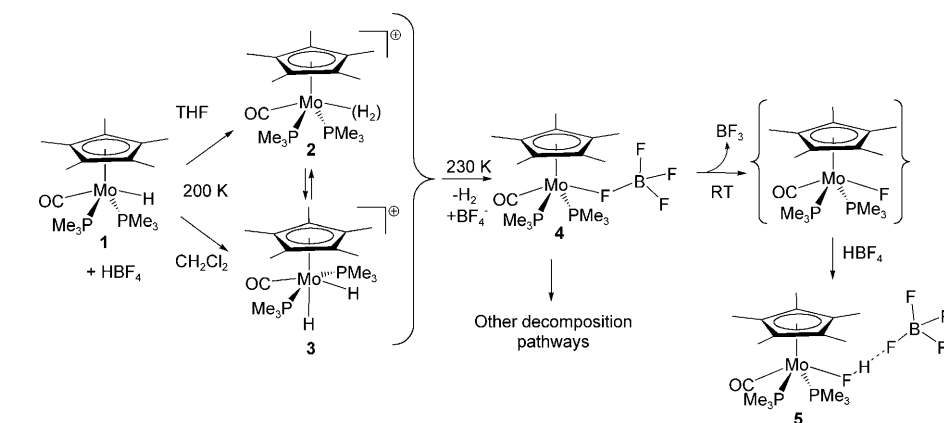
In the solid state, complex **5** displays a ν_{CO} band at 1780 cm^{−1}, that is, very close to that of compound **4**. Two ν_{BF} bands appear at 937 and 1018 cm^{−1}, accompanied by unresolved bands of lower intensity at around 1106 and 1163 cm^{−1}, in agreement with the expected lowering of the BF₄[−] symmetry. A broad band at 3477 cm^{−1} is assigned to the ν_{HF} stretching vibration. This value is substantially higher than that of the hydrogen bifluoride ion in its various salts (ν_{HF} = 1250–1750 cm^{−1})^[66] or in the above-mentioned hydrogen bifluoride complexes of transition metals (ν_{HF} = 2310–2793 cm^{−1}).^[51,52] On the other hand, it is much lower than the ν_{HF} stretching mode for free HF in the gas phase (3960 cm^{−1})^[67] or weakly bonded HF·BF₃ complex (3958 cm^{−1}),^[68] being in agreement with an HF bond elongation with respect to free HF (0.918 Å).^[51]

Discussion

Examples of tautomeric pairs of classical dihydride and dihydrogen complexes with very similar energies are rather common.^[2] In some cases, the energetic preference was shown to switch by a subtle change in the donor/acceptor and steric properties of other ligands. For instance, [Mo(CO)H₂(R₂PCH₂CH₂PR₂)₂] is a classical dihydride complex if R = Et or *i*Bu and a dihydrogen complex if R = Ph or Bz,^[69–71] whereas [W(CO)₃H₂(PR₃)₂] shows the two tautomeric forms in equilibrium if R = *i*Pr but is present exclusively as the classical dihydride if R = Me.^[72] It has been previously shown that the H–H bond in dihydrogen complexes may be very sensitive to intra- and intermolecular interactions, including ion pairing.^[73] In one case, a switch was highlighted for the same cationic complex, [Co(PP₃)H₂]⁺ (PP₃ = P(CH₂CH₂PPh₂)₃), by a mere change in counterion in the solid state; the classical dihydride structure is adopted in the presence of the BPh₄[−] anion, whereas the corresponding PF₆[−] salt reveals a nonclassical dihydrogen structure (although the positions of the two H atoms were not located).^[74] An NMR spectroscopy study, on the other hand, only reveals

the classical structure in solution.^[75,76] The example described herein, in which both cation and anion are invariant and a complete switch in solution is caused by a subtle solvent change, appears to be unprecedented.

The overall reaction of **1** with HBF₄ may be described as shown in Scheme 2. The first question to address is whether the predominant formation of **2** in THF and **3** in CH₂Cl₂ has



Scheme 2.

a kinetic or a thermodynamic origin. High activation barriers for the interconversion of classical dihydrides and dihydrogen complexes are sometimes observed when the isomerisation involves extensive ligand rearrangement. Examples are *cis*-[M(Cp*)(dppe)(η^2 -H₂)]⁺/*trans*-[M(Cp*)(dppe)H₂]⁺ (ΔH^\ddagger = 20.4(8), 20.9(8), and 21.5(10) kcal mol^{−1} for M = Fe,^[12] Ru^[13] and Os,^[77] respectively) and [W(CO)₃(η^2 -H₂)(PR₃)₂]/[W(CO)₃(H)₂(PR₃)₂] (R = cyclopentyl, ΔG^\ddagger = 11(2) kcal mol^{−1}).^[78] Theoretical investigations have shown that the [M(η^2 -H₂)]/*cis*-[M(H)₂] isomerisation has a very small barrier if the rest of the coordination sphere does not undergo significant change.^[79] The two hydride ligands in complex **3** occupy *cis* coordination sites, as shown in **I**, therefore, the rearrangement to the non-classical form must involve a very minor rearrangement of the coordination sphere. This proposition is confirmed by DFT calculations. Thus, the nature of the product is determined by thermodynamic factors. This conclusion is also consistent with the lack of observation of **2** during the thermal decomposition of **3** and with the essentially identical decomposition rate for the two isomers at the same temperature. From that rate (ca. 10^{−3} s^{−1} at 230 K), we can derive an activation free energy of 16.5 kcal mol^{−1} at 230 K for the H₂ release process, much larger than the energy barrier for the isomerisation process. Thus, the rate limiting step must be the dissociation of H₂ from **2**.

If the solvent effect is due to thermodynamics and not to kinetics, the next question to address is the origin of this effect, especially considering that THF and CH₂Cl₂ possess similar polarity (dielectric permittivity).^[80] The relative stability may be quite small, as little as 1.1 kcal mol^{−1} in favour of **2** in THF and the same amount in favour of **3** in CH₂Cl₂

(vide supra). One possibility is that the effect could be due to the ability of THF to establish hydrogen-bonding interactions as a proton acceptor with the H₂ ligand in **2** (supposedly a stronger acid than **3**), whereas dichloromethane rather displays weak proton-donating properties and prefers to interact with the BF₄[−] anion.^[20,48,81] However, the computational work suggests that the cations establish much stronger non-covalent interactions with the BF₄ counterion than with the solvent molecules. Indeed, neither CH₂Cl₂ nor THF break the [Mo(CO)(Cp*)(H₂(PMe₃)₂)]BF₄ ion pair but merely alter the cation–anion interaction in a rather minor way. Therefore, the effect of the solvent on the classical/non-classical equilibrium energetics can be described as operating through a second-order non-covalent interaction: solvent⋯anion⋯cation. The computational study, especially with the aid of calibrations by high-level MP4(SDQ) and CCSD(T), suggest that the dihydride isomer is inherently more stable than the dihydrogen complex, though by a very small margin, and that the explicit inclusion of anion and solvent molecules tilts the balance in favour of the dihydrogen complex to a greater extent in THF than in CH₂Cl₂.

The experimental observations reported herein may be compared with previously published protonation reactions of similar compounds to trace the influence of the ligand environment on the nature and stability of the protonation product. Treatment of [Mo(CO)₂(Cp)H(PMe₃)] with Et₂O·HBF₄ leads to immediate H₂ evolution, even at −78°C, in poorly coordinating or non-coordinating solvents, such as ether, toluene and heptane.^[82] In the presence of sufficiently coordinating solvents (e.g., L = MeCN), stable solvent adducts [Mo(CO)₂(Cp)(L)(PMe₃)]⁺ were obtained. The protonation of [Mo(Cp)H(PMe₃)₃]^[28] or [Mo(Cp*)H(PMe₃)₃]^[29] with HBF₄, on the other hand, leads to stable dihydride products, [Mo(H)₂(PMe₃)₃(ring)]⁺ (ring = Cp or Cp*), which shows that the metal centre in this compound is sufficiently electron-rich to prevent the formation of a (η²-H₂) complex and H₂ evolution. The present results show that an intermediate electronic environment (only one CO ligand and two PMe₃ ligands, Cp* in place of Cp) is sufficient to stabilise the primary protonation product, non-classical hydride **2** at low temperatures in THF, but not sufficient to prevent H₂ elimination at higher temperatures.

Bullock et al. have reported a low-temperature NMR spectroscopic study of the protonation of [Mo(CO)(Cp)(dppe)H]^[31] which is electronically very similar to compound **1** with TfOH. The reaction, conducted in CD₂Cl₂, led to direct formation of the dihydride product, [Mo(CO)(Cp)(dppe)(H)₂]⁺, without observation of a dihydrogen complex intermediate.^[31] This product decomposes with loss of H₂ upon warming with formation of [Mo(CO)(Cp)(dppe)(OTf)]. Like this system, compound **3** also loses H₂ upon warming with incorporation of the counterion to give **4** (Scheme 2). It is remarkable, in our opinion, that the metal in this compound prefers to accept the weakly coordinating BF₄[−] anion rather than a molecule of THF. Previously described [Mo(CO)₂(Cp)(FBBF₃)(PR₃)] analogues were apparently always handled in cold CH₂Cl₂ and the BF₄[−] ligand

was readily substituted by phosphines and olefins,^[42] but their behaviour in more coordinating solvents does not appear to have been tested. Other compounds that contain this and other weakly coordinating anions (PF₆[−], SbF₆[−], CF₃SO₃[−], etc.) have been generated in hydrocarbon solvents and the weakly coordinating anions were readily displaced under very mild conditions by a number of neutral donors, even weak ones such as R₂O.^[43] In the review by Beck and Sünkel, the affinity of [M(CO)₂(Cp)(L)]⁺ systems (M = Mo, W; L = tertiary phosphine) for Lewis bases is described as CH₂Cl₂ < BF₄[−] < THF.^[43] The different trend observed in our case for the [Mo(CO)(Cp*)(PMe₃)₂]⁺ system may be rationalised on steric grounds because the metal coordination sphere is more crowded in the present system and THF requires more space in the coordination sphere than FBF₃. The formation of complex **5** may be rationalised on the basis of the rupture of the B–F bond with loss of BF₃ from compound **4**, which is promoted by the Lewis acidity of the Mo atom, followed by trapping of the fluoride intermediate by an additional HBF₄ molecule.

Conclusions

The present investigation has shown a striking example of how delicately the ligand environment and the solvent nature control the relative stability of a classical dihydride vs. its isomeric dihydrogen complex for the protonation product of [MoH(L₃)(ring)]-type molecules. In an electron-rich ligand environment (e.g., ring = Cp or Cp* and L₃ = (PMe₃)₃), stable compounds with a classical dihydride structure are obtained. In an electron-poor environment (e.g., ring = Cp and L₃ = (CO)₂(PMe₃)), immediate decomposition occurs at 195 K, probably via a fleeting dihydrogen complex. For compound **1**, which has intermediate electronic properties, we have shown for the first time how the reaction can be steered toward the classical or the non-classical product by a small change in the solvent properties. High-level DFT calculations with the inclusion of counterion and solvent effects (through the CPCM and also through the explicit introduction of solvent molecules) have revealed intimate details of the organisation of the **2**·BF₄ and **3**·BF₄ ion pairs in solution. The solvent regulation of a classical/non-classical equilibrium with complete switch in solution, in which both cation and anion are invariant, appears to be unprecedented. The analysis reported here also reveals that a network of solvent⋯anion⋯cation non-covalent interactions is responsible for a dramatic change in the cation's nature, which demonstrates the steering role of specific solute–solvent interactions.

Experimental Section

General: All manipulations were carried out under argon. All solvents were dried over an appropriate drying agent (Na/benzophenone for toluene and THF; CaH₂ for CH₂Cl₂) and freshly distilled under argon prior

to use. C_6D_6 and $[D_8]$ toluene (Euriso-Top) were kept over molecular sieves and deoxygenated with an argon flow before use. CD_2Cl_2 and $[D_8]$ THF (Euriso-Top) were degassed by three freeze–pump–thaw cycles, then purified by vacuum transfer at RT. $[(Mo(CO)(Cp^*)H(PMe_3)_2)]$ was synthesised according to a literature procedure.^[22] $Et_2O\cdot HBF_4$ (56%, Sigma–Aldrich) was used as received.

Instrumentation: Room-temperature NMR spectroscopy was carried out by using Bruker DPX300 and AV300LiQ spectrometers operating at 300.1 (1H), 121.49 ($^{31}P\{^1H\}$) and 75.47 MHz ($^{13}C\{^1H\}$). Low-temperature 1H , $^{31}P\{^1H\}$ and $^{13}C\{^1H\}$ data were collected by using a Bruker AV500 spectrometer operating at 500.3, 202.5 and 125.8 MHz, respectively. The temperature was calibrated by using a methanol chemical shift thermometer; the accuracy and stability was ± 1 K. All samples were allowed to equilibrate for at least 3 min at every temperature. The 1H and ^{13}C spectra were calibrated by using the residual solvent signal relative to TMS and the ^{31}P was calibrated by using external 85% H_3PO_4 . The conventional inversion–recovery–pulse method (180– τ –90) was used to determine the variable-temperature longitudinal relaxation time (T_1), the calculations for which were performed by using standard Bruker software. The IR spectra were recorded by using Perkin–Elmer Spectrum 100 FTIR (2.0 cm^{-1} resolution), Specord M-82 (4.0 cm^{-1} resolution) and FT Infralum-801 (2.0 cm^{-1} resolution) spectrometers; 0.12 or 0.04 cm cells were used for the solutions.

In situ generation of compound 2 and its subsequent thermal decomposition: Compound **1** (10 mg, 0.024 mmol) and $[D_8]$ THF (0.6 mL) were added to a 5 mm NMR tube. After cooling to 200 K, a 56% solution of HBF_4 in ether (HBF_4 :ether; 3 μL , 0.70 equiv from NMR integration) was added by using a microsyringe and the reaction was directly monitored by using an NMR spectroscopic probe.

In a separate experiment, the same reaction of **1** (5 mg (0.012 mmol) and HBF_4 :ether ($\approx 1.5 \mu L$, ≈ 0.012 mmol) was carried out in regular THF (1 mL) in a Schlenk tube. The resulting solution was transferred into the IR cell inside a precooled cryostat by using a cannula, and monitored by IR spectroscopy in the ν_{CO} region.

In situ generation of compound 3 and its subsequent thermal decomposition: This experiment was run with compound **1** (10 mg, 0.024 mmol) and HBF_4 :ether (3 μL , 0.78 equiv from integration) in CD_2Cl_2 (0.6 mL) by using the same protocol as for **2**.

In a separate experiment, the same reaction was carried out by using **1** (5 mg, 0.012 mmol) and HBF_4 :ether ($\approx 1.5 \mu L$, ≈ 0.012 mmol) in CH_2Cl_2 (1 mL) in a Schlenk tube. The resulting solution was transferred into the IR cell inside a precooled cryostat by using a cannula and monitored by IR spectroscopy in the ν_{CO} region.

Generation of compound 5: HBF_4 :ether ($\approx 4.5 \mu L$, ≈ 0.035 mmol) was added by using a microsyringe to a solution of compound **1** (30 mg, 0.07 mmol) in toluene (1 mL) at RT. A pentane layer (≈ 0.5 mL) was subsequently applied to the top of the solution, which was held at $-20^\circ C$. A few crystals of compound **5** formed in two days. The amount was only sufficient to record an IR spectrum and for an X-ray structure analysis. IR (neat): $\tilde{\nu}=1780$ (s; ν_{CO}), 1091 (m), 1030 (m), 1004 (m), 936 cm^{-1} (s; BF_4).

X-ray analysis of compound 5: A single crystal was mounted under inert perfluoropolyether at the tip of a glass fibre and cooled in the cryostream of an Oxford-Diffraction XCALIBUR CCD diffractometer. Data were collected by using monochromatic MoK_{α} radiation ($\lambda=0.71073$ nm). The structure was solved by using direct methods (SIR97)^[83] and refined by least-squares procedures on F^2 by using SHELXL-97.^[84] All H atoms attached to carbon were introduced in idealised positions in the calculation and were treated as riding on their parent atoms. The two positions of the disordered H atom attached to F1 were located in the difference Fourier map and first refined by using restraints ($F-H=0.94(1)$ Å), then treated as riding on the F atom during the last stages of refinement with $U_{iso}=1.2U_{eq}(F)$. There is one well-behaved toluene solvate molecule per asymmetric unit. This molecule was located with the help of ORTEP32.^[85] Crystal data and refinement parameters are shown in Table 5. CCDC-714915 (**5**) contains the supplementary crystallographic data (excluding structure factors) for this paper. These data can be ob-

Table 5. Crystal data and structure refinement for **5**· $C_6H_5CH_3$.^[a]

	5 · $C_6H_5CH_3$
empirical formula	$C_{24}H_{42}BF_5MoOP_2$
M_r	610.27
crystal colour, habit	dark violet, box
crystal system	monoclinic
crystal size [mm]	$0.54 \times 0.32 \times 0.16$
T [K]	180(2)
space group	$P2_1/a$
a [Å]	9.6293(3)
b [Å]	26.8813(7)
c [Å]	11.3274(3)
β [°]	100.553(3)
V [Å ³]	2882.48(14)
Z	4
ρ_{calcd} [g cm ⁻³]	1.406
μ [mm ⁻¹]	0.613
min/max transmission	0.43366/1.000
θ range [°]	32.12
$F(000)$	1264
reflms measured	30896
independent reflms (R_{int})	9529 (0.0438)
completeness of dataset [%]	94.3
observed reflms [$I > 2\sigma(I)$]	5715
parameters	319
GOF	0.984
R_1, wR_2 [$I > 2\sigma(I)$]	0.0355, 0.0810
R_1, wR_2 (all data)	0.0789, 0.0996
$\Delta\rho_{min}, \Delta\rho_{max}$ [e Å ⁻³]	1.191, -0.900

[a] Only the average values are given for chemically equivalent parameters. [b] From reference [96].

tained free of charge from The Cambridge Crystallographic Data Centre via www.ccdc.cam.ac.uk/data_request/cif.

Computational details: All calculations were performed at the DFT level by using the M05-2X functional^[36] and the hybrid B3LYP functional,^[86–88] as implemented in Gaussian 03.^[89] The optimisations of the dihydrogen/dihydride cations, the ion pairs with the BF_4^- counterion and the adducts containing one solvent molecule were also performed at the DFT/B3PW91 and MP2 levels. The MP4(SDQ) and CCSD(T) methods were used for single-point calculations at the MP2-optimised geometry of the model $[Mo(CO)(Cp)(H)_2(PH_3)_2]^+$ complexes. The basis set for the Mo and P atoms was that associated with the pseudopotential^[90,91] with a standard double- ζ LANL2DZ contraction,^[89] supplemented in the case of P with a set of d-polarisation functions.^[92] The 6-31G(d) basis set was used for C atoms of Cp^* ring and CH_2Cl_2 , and for B and F atoms of BF_4 . The 6-31++G(d,p) basis set was used for the CO group, the hydride ligands, the O atom of THF, the CH_2Cl_2 chlorine atoms and the acidic H atoms of HBF_4 and CH_2Cl_2 . The 6-31G basis set was used for all other atoms. The structures of the reactants, intermediates, transition states and products were fully optimised without any symmetry restrictions. Transition states were identified as having one imaginary frequency in the Hessian matrix. No scaling factor was applied to the calculated frequencies because the optimisation was run in the gas phase and the IR spectra were measured in solution. The average ratio between the experimental and calculated ν_{CO} values is around 0.95. Non-specific solvent effects were introduced through CPCM representation of the solvent by single-point calculations^[93,94] on gas-phase-optimised geometries for dichloromethane ($\epsilon=8.93$) and THF ($\epsilon=7.58$). The ΔE^{solv} and ΔG^{solv} values were obtained by adding the contribution of the free energy of solvation to the gas-phase potential energy and gas-phase free energy, respectively.^[95] Specific solvent effects in the ion pairs were considered by introducing discrete solvent molecules (either CH_2Cl_2 or THF) to solvate the BF_4 anion of the ion pair. To generate good starting points for the optimisation of the solvated ion pairs, the most stable conformation of the solvated free BF_4 anion was initially investigated. Then the calculated arrange-

ment of solvent molecules was introduced into the most stable conformations of the ion-pairs and the system was fully optimised.

Acknowledgements

Support of this work through two bilateral programs (France–Russia: PICS grant 2004–07 continuing within the framework of a GDRE (groupe de recherche européen) 2008–11; France–Spain: LEA-CTPMM) is gratefully acknowledged. Additional national support was obtained in France from the CNRS, the IUF, and the CICT (project CALMIP), in Russia from the RFBR (08-03-00464), the Division of Chemistry and Material Sciences of RAS and the Russian Federation President grant (MK-380.2008.3) and in Spain from MICINN (projects CTQ2008-06669-C02-01 and Consolider Ingenio 2010 CSD2007-00006). O.A.F. thanks INTAS for an individual YSF grant (No 06-1000014-5809). Thanks are also expressed to Dr. Y. Coppel (LCC CNRS) for assistance with the low-temperature NMR spectroscopy.

- [1] G. J. Kubas, R. R. Ryan, B. I. Swanson, P. J. Vergamini, H. J. Wassermann, *J. Am. Chem. Soc.* **1984**, *106*, 451–452.
- [2] G. J. Kubas, *Metal Dihydrogen and σ -Bond Complexes*, Kluwer Academic/Plenum Press, New York, **2001**.
- [3] M. A. Esteruelas, L. A. Oro, *Chem. Rev.* **1998**, *98*, 577–588.
- [4] N. K. Szymczak, D. R. Tyler, *Coord. Chem. Rev.* **2008**, *252*, 212–230.
- [5] C. P. Lau, S. M. Ng, G. Jia, Z. Lin, *Coord. Chem. Rev.* **2007**, *251*, 2223–2237.
- [6] G. J. Kubas, *Chem. Rev.* **2007**, *107*, 4152–4205.
- [7] G. J. Kubas, *Acc. Chem. Res.* **1988**, *21*, 120–128.
- [8] P. G. Jessop, R. H. Morris, *Coord. Chem. Rev.* **1992**, *121*, 155–284.
- [9] P. Hamon, L. Toupet, J.-R. Hamon, C. Lapinte, *Organometallics* **1992**, *11*, 1429–1431.
- [10] N. V. Belkova, P. O. Revin, L. M. Epstein, E. V. Vorontsov, V. I. Bakhmutov, E. S. Shubina, E. Collange, R. Poli, *J. Am. Chem. Soc.* **2003**, *125*, 11106–11115.
- [11] N. V. Belkova, E. Collange, P. Dub, L. M. Epstein, D. A. Lemenovskii, A. Lledós, A. Maresca, F. Maseras, R. Poli, P. O. Revin, E. S. Shubina, E. V. Vorontsov, *Chem. Eur. J.* **2005**, *11*, 873–888.
- [12] M. Baya, O. Maresca, R. Poli, Y. Coppel, F. Maseras, A. Lledós, N. V. Belkova, P. A. Dub, L. M. Epstein, E. S. Shubina, *Inorg. Chem.* **2006**, *45*, 10248–10262.
- [13] N. V. Belkova, P. A. Dub, M. Baya, J. Houghton, *Inorg. Chim. Acta* **2007**, *360*, 149–162.
- [14] P. A. Dub, N. V. Belkova, K. A. Lyssenko, G. A. Silantyev, L. M. Epstein, E. S. Shubina, J.-C. Daran, R. Poli, *Organometallics* **2008**, *27*, 3307–3311.
- [15] M. Besora, A. Lledós, F. Maseras, *Chem. Soc. Rev.* **2009**, *38*, 957–966.
- [16] S. Gründemann, S. Ulrich, H.-H. Limbach, N. S. Golubev, G. S. Denisov, L. M. Epstein, S. Sabo-Etienne, B. Chaudret, *Inorg. Chem.* **1999**, *38*, 2550–2551.
- [17] M. G. Basallote, M. Feliz, M. J. Fernandez-Trujillo, R. Llusar, V. S. Safont, S. Uriel, *Chem. Eur. J.* **2004**, *10*, 1463–1471.
- [18] A. G. Algarra, M. G. Basallote, M. Feliz, M. J. Fernandez-Trujillo, R. Llusar, V. S. Safont, *Chem. Eur. J.* **2006**, *12*, 1413–1426.
- [19] N. Belkova, M. Besora, L. Epstein, A. Lledós, F. Maseras, E. Shubina, *J. Am. Chem. Soc.* **2003**, *125*, 7715–7725.
- [20] N. V. Belkova, T. N. Gribanova, E. I. Gutsul, R. M. Minyaev, C. Bianchini, M. Peruzzini, F. Zanobini, E. S. Shubina, L. M. Epstein, *J. Mol. Struct.* **2007**, *844*, 115–131.
- [21] P. A. Dub, M. Baya, J. Houghton, N. V. Belkova, J. C. Daran, R. Poli, L. M. Epstein, E. S. Shubina, *Eur. J. Inorg. Chem.* **2007**, 2813–2826.
- [22] J. H. Shin, D. G. Churchill, G. Parkin, *J. Organomet. Chem.* **2002**, *642*, 9–15.
- [23] NMR spectroscopic properties of $[\text{MoCl}(\text{CO})(\text{Cp}^*)(\text{PMe}_3)_2]$: ^1H NMR (500 MHz, CD_2Cl_2): $\delta = 1.81$ (s, 15H, Cp^*), 1.41 ppm (d, 18H, $^2J(\text{H,P}) = 8$ Hz); $^{31}\text{P}\{^1\text{H}\}$ NMR (500 MHz, CD_2Cl_2): $\delta = 17.9$ ppm (s).
- [24] P. J. Desrosiers, L. Cai, Z. Lin, R. Richards, J. Halpern, *J. Am. Chem. Soc.* **1991**, *113*, 4173–4184.
- [25] M. T. Bautista, K. A. Earl, P. A. Maltby, R. H. Morris, C. T. Schweitzer, A. Sella, *J. Am. Chem. Soc.* **1988**, *110*, 7031–7036.
- [26] L. M. Epstein, N. V. Belkova, E. I. Gutsul, E. S. Shubina, *Polish J. Chem.* **2003**, *77*, 1371–1383.
- [27] R. M. Bullock, J.-S. Song, D. J. Szalda, *Organometallics* **1996**, *15*, 2504–2516.
- [28] J. C. Fetting, H.-B. Kraatz, R. Poli, E. A. Quadrelli, R. C. Torralba, *Organometallics* **1998**, *17*, 5767–5775.
- [29] M. Baya, P. A. Dub, J. Houghton, J.-C. Daran, R. Poli, N. V. Belkova, E. S. Shubina, L. M. Epstein, A. Lledós, *Inorg. Chem.* **2009**, *48*, 209–220.
- [30] M. L. H. Green, A. K. Hughes, P. Lincoln, J. J. Martin-Polo, P. Mountford, A. Sella, L.-L. Wong, J. A. Bandy, T. W. Banks, K. Prout, D. J. Watkin, *J. Chem. Soc. Dalton Trans.* **1992**, 2063–2069.
- [31] T.-Y. Cheng, D. J. Szalda, J. Zhang, R. M. Bullock, *Inorg. Chem.* **2006**, *45*, 4712–4720.
- [32] N. Legrand, A. Bondon, G. Simonneaux, C. Jung, E. Gill, *FEBS Lett.* **1995**, *364*, 152–156.
- [33] W. T. Potter, J. H. Hazzard, M. G. Choc, M. P. Tucker, W. S. Caughey, *Biochemistry* **1990**, *29*, 6283–6295.
- [34] J. W. Box, G. M. Gray, *Magn. Reson. Chem.* **1986**, *24*, 527–533.
- [35] J. W. Box, G. M. Gray, *Inorg. Chem.* **1987**, *26*, 2774–2778.
- [36] Y. Zhao, N. E. Schultz, D. G. Truhlar, *J. Chem. Theory Comput.* **2006**, *2*, 364–382.
- [37] Y. Zhao, D. G. Truhlar, *Theor. Chem. Acc.* **2008**, *120*, 215–241.
- [38] After inclusion of the BF_4^- counterion, these alternative geometries are even higher than the global minimum (> 10 kcal mol $^{-1}$).
- [39] M. G. Basallote, J. Durán, M. J. Fernández-Trujillo, M. A. Máñez, *Organometallics* **2000**, *19*, 695–698.
- [40] M. R. Colman, T. D. Newbound, L. J. Marschall, M. D. Noirot, M. M. Miller, G. P. Wulfsberg, J. S. Frye, O. P. Anderson, S. H. Strauss, *J. Am. Chem. Soc.* **1990**, *112*, 2349–2362.
- [41] S. H. Strauss, *Chemtracts: Inorg. Chem.* **1994**, *6*, 1–13.
- [42] K. Sünkel, H. Ernst, W. Beck, *Z. Naturforsch. B* **1981**, *36*, 474–481.
- [43] W. Beck, K. Sünkel, *Chem. Rev.* **1988**, *88*, 1405–1421.
- [44] K. Sünkel, G. Urban, W. Beck, *J. Organomet. Chem.* **1983**, *252*, 187–194.
- [45] W. H. Hersh, *J. Am. Chem. Soc.* **1985**, *107*, 4599–4601.
- [46] R. V. Honeychuck, W. H. Hersh, *Inorg. Chem.* **1989**, *28*, 2869–2886.
- [47] L. S. Van Der Sluis, K. A. Kubat-Martin, G. J. Kubas, K. G. Caulton, *Inorg. Chem.* **1991**, *30*, 306–310.
- [48] A. Allerhand, P. V. Schleyer, *J. Am. Chem. Soc.* **1963**, *85*, 1715–1723.
- [49] M. Appel, W. Beck, *J. Organomet. Chem.* **1987**, *319*, C1–C4.
- [50] V. J. Murphy, T. Hascall, J. Y. Chen, G. Parkin, *J. Am. Chem. Soc.* **1996**, *118*, 7428–7429.
- [51] V. J. Murphy, D. Rabinovich, T. Hascall, W. T. Klooster, T. F. Koetzle, G. Parkin, *J. Am. Chem. Soc.* **1998**, *120*, 4372–4387.
- [52] N. A. Jasim, R. N. Perutz, S. P. Foxon, P. H. Walton, *J. Chem. Soc. Dalton Trans.* **2001**, 1676–1685.
- [53] M. K. Whittlesey, R. N. Perutz, B. Greener, M. H. Moore, *Chem. Commun.* **1997**, 187–188.
- [54] J. Vicente, J. Gil-Rubio, D. Bautista, A. Sironi, N. Masciocchi, *Inorg. Chem.* **2004**, *43*, 5665–5675.
- [55] D. C. Roe, W. J. Marshall, F. Davidson, P. D. Soper, V. V. Grushin, *Organometallics* **2000**, *19*, 4575–4582.
- [56] T. Chandler, G. R. Kriek, A. M. Greenaway, J. H. Enemark, *Cryst. Struct. Commun.* **1980**, *9*, 557–562.
- [57] S. J. N. Burgmayer, J. L. Templeton, *Inorg. Chem.* **1985**, *24*, 2224–2230.
- [58] R. Ellis, R. A. Henderson, A. Hills, D. L. Hughes, *J. Organomet. Chem.* **1987**, *333*, C6–C10.
- [59] J. J. R. Fraústo da Silva, M. A. Pellinghelli, A. J. L. Pombeiro, R. L. Richards, A. Tiripicchio, Y. Wang, *J. Organomet. Chem.* **1993**, *C8*–C10.

- [60] Y. Wang, J. J. R. Fraústo Da Silva, A. J. L. Pombeiro, M. A. Pellinghelli, A. Tiripicchio, R. A. Henderson, R. L. Richards, *J. Chem. Soc. Dalton Trans.* **1995**, 1183–1191.
- [61] F. V. Cochran, P. J. Bonitatebus, R. R. Schrock, *Organometallics* **2000**, *19*, 2414–2416.
- [62] L. Coue, L. Cuesta, D. Morales, J. A. Halfen, J. Perez, L. Riera, V. Riera, D. Miguel, N. G. Connelly, S. Boonyuen, *Chem. Eur. J.* **2004**, *10*, 1906–1912.
- [63] Z. Mazej, H. Borrmann, K. Lutar, B. Zemva, *Inorg. Chem.* **1998**, *37*, 5912–5914.
- [64] D. H. Lee, H. J. Kwon, P. P. Patel, L. M. Liable-Sands, A. L. Rheingold, R. H. Crabtree, *Organometallics* **1999**, *18*, 1615–1621.
- [65] E. Clot, O. Eisenstein, R. H. Crabtree, *New J. Chem.* **2001**, *25*, 66–72.
- [66] B. S. Ault, *Acc. Chem. Res.* **1982**, *15*, 103–109.
- [67] D. G. Tuck, *Prog. Inorg. Chem.* **1967**, *9*, 161–194.
- [68] K. Nauta, R. E. Miller, G. T. Fraser, W. J. Lafferty, *Chem. Phys. Lett.* **2000**, *322*, 401–406.
- [69] G. J. Kubas, R. R. Ryan, D. A. Wroblewski, *J. Am. Chem. Soc.* **1986**, *108*, 1339–1341.
- [70] G. J. Kubas, R. R. Ryan, C. J. Unkefer, *J. Am. Chem. Soc.* **1987**, *109*, 8113–8115.
- [71] G. J. Kubas, C. J. Burns, J. Eckert, S. W. Johnson, A. C. Larson, P. J. Vergamini, C. J. Unkefer, G. R. K. Khalsa, S. A. Jackson, O. Eisenstein, *J. Am. Chem. Soc.* **1993**, *115*, 569–581.
- [72] G. J. Kubas, *Comments Inorg. Chem.* **1988**, *7*, 17–40.
- [73] D. G. Gusev, *J. Am. Chem. Soc.* **2004**, *126*, 14249–14257.
- [74] C. Bianchini, C. Mealli, M. Peruzzini, F. Zanobini, *J. Am. Chem. Soc.* **1992**, *114*, 5905–5906.
- [75] D. M. Heinekey, A. Liegeois, M. Van Roon, *J. Am. Chem. Soc.* **1994**, *116*, 8388–8389.
- [76] D. M. Heinekey, M. Van Roon, *J. Am. Chem. Soc.* **1996**, *118*, 12134–12140.
- [77] P. A. Dub, N. V. Belkova, O. A. Fillipov, G. A. Silantyev, J.-C. Daran, L. M. Epstein, R. Poli, E. S. Shubina, unpublished results.
- [78] G. R. K. Khalsa, G. J. Kubas, C. J. Unkefer, L. S. Van Der Sluys, K. A. Kubat-Martin, *J. Am. Chem. Soc.* **1990**, *112*, 3855–3860.
- [79] F. Maseras, A. Lledós, E. Clot, O. Eisenstein, *Chem. Rev.* **2000**, *100*, 601–636.
- [80] C. Reichardt, *Solvents and Solvent Effects in Organic Chemistry*, Wiley-VCH, Weinheim, **2003**.
- [81] A. Fujii, K. Shibasaki, T. Kazama, R. Itaya, N. Mikami, S. Tsuzuki, *Phys. Chem. Chem. Phys.* **2008**, *10*, 2836–2843.
- [82] E. A. Quadrelli, H.-B. Kraatz, R. Poli, *Inorg. Chem.* **1996**, *35*, 5154–5162.
- [83] A. Altomare, M. Burla, M. Camalli, G. Cascarano, C. Giacovazzo, A. Guagliardi, A. Moliterni, G. Polidori, R. Spagna, *J. Appl. Crystallogr.* **1999**, *32*, 115–119.
- [84] SHELXL97, program for crystal structure refinement, G. M. Sheldrick, University of Göttingen, Göttingen, **1997**.
- [85] L. J. Farrugia, *J. Appl. Crystallogr.* **1997**, *30*, 565.
- [86] A. D. Becke, *J. Chem. Phys.* **1993**, *98*, 5648–5652.
- [87] C. T. Lee, W. T. Yang, R. G. Parr, *Phys. Rev. B* **1988**, *37*, 785–789.
- [88] P. Stephens, F. Devlin, C. Chabalowski, M. Frisch, *J. Phys. Chem.* **1994**, *98*, 11623–11627.
- [89] Gaussian 03, Revision D.01, M. J. Frisch, G. W. Trucks, H. B. Schlegel, G. E. Scuseria, M. A. Robb, J. R. Cheeseman, J. Montgomery, Jr., J. A., T. Vreven, K. N. Kudin, J. C. Burant, J. M. Millam, S. S. Iyengar, J. Tomasi, V. Barone, B. Mennucci, M. Cossi, G. Scalmani, N. Rega, G. A. Petersson, H. Nakatsuji, M. Hada, M. Ehara, K. Toyota, R. Fukuda, J. Hasegawa, M. Ishida, T. Nakajima, Y. Honda, O. Kitao, H. Nakai, M. Klene, X. Li, J. E. Knox, H. P. Hratchian, J. B. Cross, C. Adamo, J. Jaramillo, R. Gomperts, R. E. Stratmann, O. Yazyev, A. J. Austin, R. Cammi, C. Pomelli, J. W. Ochterski, P. Y. Ayala, K. Morokuma, G. A. Voth, P. Salvador, J. J. Dannenberg, V. G. Zakrzewski, S. Dapprich, A. D. Daniels, M. C. Strain, O. Farkas, D. K. Malick, A. D. Rabuck, K. Raghavachari, J. B. Foresman, J. V. Ortiz, Q. Cui, A. G. Baboul, S. Clifford, J. Cioslowski, B. B. Stefanov, G. Liu, A. Liashenko, P. Piskorz, I. Komaromi, R. L. Martin, D. J. Fox, T. Keith, M. A. Al-Laham, C. Y. Peng, A. Nanayakkara, M. Challacombe, P. M. W. Gill, B. Johnson, W. Chen, M. W. Wong, C. Gonzalez, J. A. Pople, Gaussian, Inc., Wallingford CT, **2004**.
- [90] P. J. Hay, W. R. Wadt, *J. Chem. Phys.* **1985**, *82*, 270–283.
- [91] W. R. Wadt, P. J. Hay, *J. Chem. Phys.* **1985**, *82*, 284–298.
- [92] A. Höllwarth, M. Böhme, S. Dapprich, A. Ehlers, A. Gobbi, V. Jonas, K. Kohler, R. Stegmann, A. Veldkamp, G. Frenking, *Chem. Phys. Lett.* **1993**, *208*, 237–240.
- [93] V. Barone, M. Cossi, *J. Phys. Chem. A* **1998**, *102*, 1995–2001.
- [94] M. Cossi, N. Rega, G. Scalmani, V. Barone, *J. Comput. Chem.* **2003**, *24*, 669–681.
- [95] A. A. C. Braga, G. Ujaque, F. Maseras, *Organometallics* **2006**, *25*, 3647–3658.
- [96] R. C. Elder, *Inorg. Chem.* **1968**, *7*, 1117–1123.

Received: June 13, 2009
Published online: November 5, 2009